Selective-area vapor-liquid-solid growth of tunable InAsP quantum dots

Dalacu, Dan; Mnaymneh, Khaled; Wu, Xiaohua; Lapointe, Jean; Aers, Geof C.; Poole, Philip J.; Williams, Robin L.

Publisher's version / Version de l'éditeur:
https://doi.org/10.1063/1.3600777
Applied Physics Letters, 98, 25, p. 251101, 2011-06-20

Selective-area vapor-liquid-solid growth of tunable InAsP quantum dots in nanowires

Dan Dalacu,[a] Khaled Mnaymneh, Xiaohua Wu, Jean Lapointe, Geof C. Aers, Philip J. Poole, and Robin L. Williams
Institute for Microstructural Sciences, National Research Council, Ottawa K1A 0R6, Canada

(Received 19 April 2011; accepted 27 May 2011; published online 20 June 2011)

A process is described where the position, size, and cladding of an InP nanowire with an embedded InAsP quantum dot are determined by design through lithography, processing, and growth. The vapor-liquid-solid growth mode on a patterned substrate is used to grow the InP core and defines the quantum dot size to better than ±2 nm while selective-area growth is used to define the cladding thickness. The clad nanowires emit efficiently in the range $\lambda = 0.95-1.15$ μm. Photoluminescence measurements are used to quantify the dependence of the excitonic energy level structure on quantum dot size for diameters 10–40 nm. [doi:10.1063/1.3600777]

The conventional approach to fabricating efficient single photon sources based on self-assembled quantum dots has been to use high finesse microcavities, taking advantage of the Purcell effect[1] to efficiently channel photons from an excitonic decay into a resonant mode of the cavity.[2] Recently, a highly efficient single photon source has been demonstrated in a photonic wire,[3] essentially an axial waveguide with a geometry similar to a small diameter micropillar cavity[4] without Bragg mirrors. The devices are fabricated from a planar GaAs layer containing an ensemble of Stranski–Krastanow self-assembled InAs quantum dots using the standard top-down approach whereby the photonic wires are defined through electron beam lithography and dry-etching.

Quantum dots in nanowires, such as self-assembled dots, form a strongly confined system with narrow transition linewidths[5,6] useful for single photon[7] and entangled photon pair generation.[8] Unlike self-assembled dots in etched photonic wires, quantum dots in nanowires are grown, damage-free, from the bottom up via vapor-liquid-solid (VLS) (Refs. 9 and 10) or selective area[11,12] epitaxy. More importantly, each nanowire contains a single quantum dot which is naturally located on the axis of the nanowire for maximum coupling to the optical field of the waveguide.

For scalable implementations of nanowire-based single photon sources,[8,13] VLS nanowires can be positioned using a standard metal lift-off process[10] while positioning of selective-area nanowires is inherent to the growth mode.[11,12] In this letter, we address two additional aspects for complete control of nanowire-based photonic wires; quantum dot size and cladding geometry. Using VLS epitaxy on a patterned substrate, the diameter of the catalyst is controlled through electron-beam lithography to better than ±2 nm. With the patterned-substrate, one can switch from VLS to selective-area growth, where the latter is used to clad the nanowire. The cladding of the nanowire is a crucial aspect of the device performance,[13–15] and the approach adopted here can potentially be used to grow photonic wires with an optimal geometry for photon extraction.[16]

The nanowires are based on the InAs/InP material system. A (111)B S-doped InP substrate is coated with a 20 nm SiO_2 mask that is electron beam patterned to produce an array of holes, 30 to 90 nm in diameter, that will define the gold catalyst size. The substrate is then wet etched in a buffered HF solution to produce openings in the SiO_2 that will define the cladding of the nanowire. The diameter of these holes is set by the etch time, with the isotropic HF etch producing an undercut profile shown schematically in Fig. 1(a). A standard metal lift-off process is used to deposit 10 nm (samples A and B) or 1 nm (sample C) of gold in the center of the opening in the oxide resulting in gold catalyst diameters of $d = 20-40$ nm or $d = 10-16$ nm, respectively, as measured after growth. A plan view scanning electron microscopy (SEM) image of a catalyst prior to growth is shown in Fig. 1(b).

The nanowires are grown using chemical beam epitaxy with trimethylindium (TMI) and precracked PH_3 and AsH_3. The initial growth, which defines the quantum dot size, is carried out in the VLS mode at 450 °C. At this temperature, InP grows exclusively at the gold–InP interface with no growth occurring in the annulus of exposed InP around the gold particle nor on the oxide-covered substrate[17] as shown in Fig. 2(a). The crystalline structure of all the InP nanowires were predominantly wurtzite [see Fig. 2(b)] with a growth rate-dependent stacking fault density. The VLS growth on patterned substrates is highly reproducible [see Fig. 1(c)]

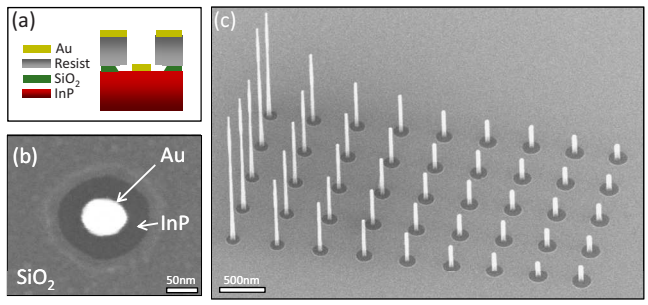

FIG. 1. (Color online) (a) Schematic illustration of the self-aligned lift-off process used to position gold catalysts in circular openings of a SiO_2 mask. (b) Plan view SEM image of a positioned gold catalyst 70 nm in diameter prior to growth. (c) SEM image of an array of InP nanowires where the size of the gold catalyst is increased from left ($d = 20$ nm) to right ($d = 40$ nm) with a corresponding decrease in height due to a nonlinear diameter-dependent growth rate.

[a]Electronic mail: dan.dalacu@nrc-cnrc.gc.ca.

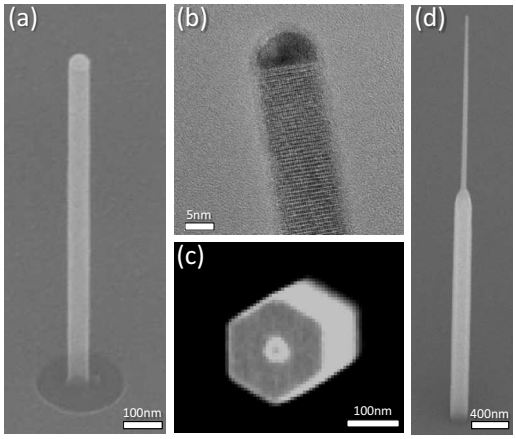

FIG. 2. (a) SEM image of a $d=40$ nm InP nanowire prior to cladding. The nanowire is untapered, and the diameter of the gold catalyst is used as a measure of the lateral size of the InAsP quantum dot embedded at the base of the wire. (b) Scanning transmission electron microscopy image of an InP nanowire with a wurtzite crystalline structure. (c) and (d) show a clad nanowire in plan view and at 45°, respectively. The clad nanowire has a diameter of $d=175$ nm with clearly delineated faceted sidewalls.

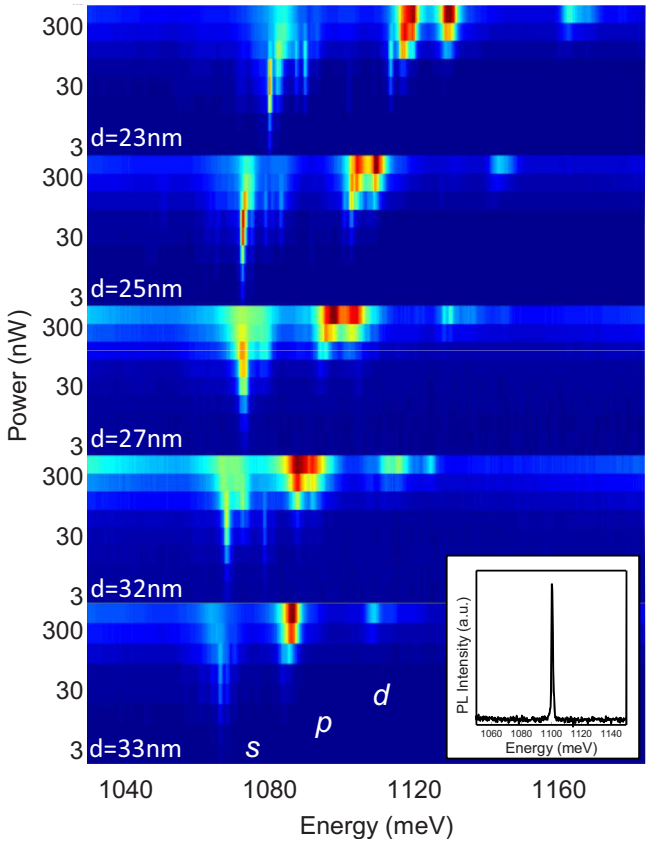

FIG. 3. (Color online) Power-dependent emission spectra for a series of nanowires as a function of catalyst diameter. The diameters are obtained from SEM images of the measured nanowires. The inset shows the ground state emission of a $d=22.8$ nm nanowire.

with nanowire diameters controlled to ±2 nm. The size of the gold catalysts increases from left to right in nominally 2 nm increments with a corresponding decrease in nanowire height from the catalyst size-dependent growth rate.[17] InAsP quantum dots are incorporated at the base of the nanowires, 300–500 nm from the substrate surface, by switching from PH_3 to AsH_3 for two seconds. The quantum dots in sample A were grown with a TMI flux during the AsH_3 exposure, while the dots in sample B and C were grown without TMI present. Figure 2(a) shows a 1 μm nanowire with an InAsP quantum dot located roughly in the middle. Nanowires this tall are untapered, and the diameter of the gold catalyst is a good measure of the lateral size of the embedded quantum dot.

To grow the cladding, the growth temperature is raised to 515 °C. At this temperature, the VLS growth mode is turned off and the noncatalyzed growth mode on the InP substrate is turned on.[17] Growth of the cladding material simply proceeds by filling in the annulus around the nanowire core, the diameter of which is determined by processing. A clad nanowire is shown in Figs. 2(c) and 2(d). The cladding extends half way up the nanowire, and reveals the crystalline facets of the wurtzite structure oriented along the ⟨110⟩ directions of the (111) substrate. The diameter of the cladded region is $d=175$ nm, lower than the optimal $d=250$ nm based on calculations in Ref. 16 taking into account the lower index of refraction of InP compared to GaAs. The nanowires for optical study are grown sufficiently long to promote some tapering in the tip region due to finite indium diffusion lengths on the sidewall facets.[17] The taper is another aspect in the design of an efficient device.[16]

Optical measurements on individual nanowires were performed at 5 K in a continuous flow helium cryostat using nonresonant, above band gap excitation through a microscope objective. The photoluminescence (PL) is collected through the same microscope objective, dispersed using a single grating spectrometer and detected using a liquid-nitrogen cooled InGaAs diode array. After the PL measurements, the same nanowires are imaged in a SEM to determine the diameter of the gold catalyst which is used as a measure of the quantum dot lateral size.

Figure 3 shows the power-dependent spectra of five nanowires with quantum dot diameters of $d=23$ nm to $d=33$ nm. For each nanowire, the ground state emission is a single peak with linewidths of a few hundreds of microelectronvolt. A typical spectrum pumped at saturation is shown in the inset of Fig. 3. The linewidth is 400 μeV and the photon count rate is 500 cts/s, similar to InAs/InP self-assembled quantum dots. The spectra at higher pump powers display bound s, p, and d shells. As the dot size is decreased, the level spacings increase[15] in accordance with increased lateral confinement. We emphasis that the quantum dot size is determined by design through lithography, and that the spectra in Fig. 3 are obtained from adjacent nanowires positioned in an array similar to that in Fig. 1(b) with nominal 2 nm increments in the diameter of the quantum dot.

Ground state emission energies and s to p level splittings are plotted as a function of quantum dot diameter in Fig. 4. For quantum dot sizes less than $d\sim 24$ nm, the ground state energy blueshifts with decreasing size at a rate of ~ 17 meV/nm. A similar ground state dependence on quantum dot size has been previously observed.[15] This trend is opposite to that expected from the known growth rate behavior as a function of nanowire diameter (for sample A), described in Ref. 17. The growth rate for a large diameter nanowire is smaller than for a small diameter wire, and thus larger diameter wires should have thinner quantum dots with a corresponding increase in ground state energy. Countering this effect is the decrease in lateral confinement with increasing

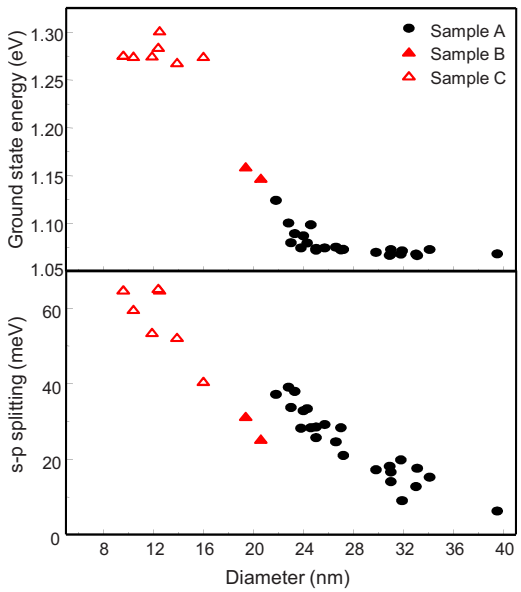

FIG. 4. (Color online) (a) Ground state emission energy and (b) $s-p$ level splitting as a function of quantum dot diameter. The dots are formed by switching the PH_3/AsH_3 out of/into the growth chamber simultaneously for 2 s, sample A with indium supplied, samples B and C without.

nanowire diameter but this is not strong enough to explain our results. For samples B and C there is no indium supplied during the AsH_3 exposure and the dots are grown in the manner explained in Ref. 18. In that reference, when growing InP the Au particle contained 44% In, and for InAs growth it contained 34% In. When switching from a P to an As ambient the extra 10% In in the Au particle was expelled through the growth of an InAs layer until a concentration of 34% was reached. This means that an InAs layer can be grown without injecting an indium source into the growth chamber. If a fixed change in In concentration in the Au particle is obtained then the thickness of the InAs layer will be directly proportional to the nanowire diameter. This is the correct trend for the behavior observed in our samples.

The splittings between the ground and first excited state as a function of quantum dot size are shown in Fig. 4(b) and are consistent with the results of Ref. 15. The observed increase in the $s-p$ splitting for decreased diameters is expected from a first order single-band approximation where the energy separation between s and p levels of quantum dots strongly confined in the growth direction is determined by the lateral size of the dot.

In conclusion, we combine VLS and selective-area epitaxy to grow InP nanowires with embedded InAsP quantum dots where the core wire and cladding thickness are defined independently by switching between growth modes. The quantum dot diameter is tuned in a controlled manner from 10 to 40 nm in 2 nm increments. The corresponding decrease in lateral confinement manifests in a decrease in the s to p level splittings, from 65 to 6 meV, illustrating the high level of control possible with nanowire-based quantum dots. The ability to control, by design, the nanowire position, diameter, and cladding thickness is relevant to the scalability, tunability, and emission efficiency, respectively, of nanowire-based photon sources.

[1]E. M. Purcell, Phys. Rev. **69**, 37 (1946).
[2]A. J. Shields, Nat. Photonics **1**, 215 (2007).
[3]J. Claudon, J. Bleuse, N. S. Malik, M. Bazin, P. Jaffrennou, N. Gregersen, C. Sauvan, P. Lalanne, and J.-M. Gérard, Nat. Photonics **4**, 174 (2010).
[4]E. Moreau, J. M. Gérard, I. Bram, L. Manin, and V. Thierry-Mieg, Appl. Phys. Lett. **79**, 2865 (2001).
[5]N. Panev, A. I. Persson, N. Sköld, and L. Samuelson, Appl. Phys. Lett. **83**, 2238 (2003).
[6]M. H. M. van Weert, N. Akopian, U. Perinetti, M. P. van Kouwen, R. E. Algra, M. A. Verheijen, E. P. A. M. Bakkers, L. P. Kouwenhoven, and V. Zwiller, Nano Lett. **9**, 1989 (2009).
[7]M. Borgström, V. Zwiller, E. Müller, and A. Imamoglu, Nano Lett. **5**, 1439 (2005).
[8]S. N. Dorenbos, H. Sasakura, M. P. van Kouwen, N. Kopian, S. Adachi, N. Namekata, M. Jo, J. Motohisa, Y. Kobayashi, K. Tomioka, T. Fukui, S. Inoue, H. Kumano, C. M. Natarajan, R. H. Hadfield, T. Zijlstra, T. M. Klapwijk, V. Zwiller, and I. Suemune, Appl. Phys. Lett. **97**, 171106 (2010).
[9]R. S. Wagner and W. C. Ellis, Appl. Phys. Lett. **4**, 89 (1964).
[10]L. E. Jensen, S. J. M. T. Björk, A. I. Persson, B. J. Ohlsson, and L. Samuelson, Nano Lett. **4**, 1961 (2004).
[11]P. J. Poole, J. Lefebvre, and J. Fraser, Appl. Phys. Lett. **83**, 2055 (2003).
[12]P. Mohan, J. Motohisa, and T. Fukui, Nanotechnology **16**, 2903 (2005).
[13]J. Heinrich, A. Hugenberger, T. Heindel, S. Reitzenstein, S. Höfling, L. Worschech, and A. Forchel, Appl. Phys. Lett. **96**, 211117 (2010).
[14]M. Tchernycheva, G. E. Cirlin, G. Patriarche, L. Travers, V. Zwiller, U. Perinetti, and J.-C. Harmand, Nano Lett. **7**, 1500 (2007).
[15]N. Sköld, M.-K. Pistol, K. A. Dick, C. Pryor, J. B. Wagner, L. S. Karlsson, and L. Samuelson, Phys. Rev. B **80**, 041312(R) (2009).
[16]I. Friedler, C. Sauvan, J. P. Hugonin, P. Lalanne, J. Claudon, and J. M. Gerard, Opt. Exp. **17**, 2095 (2009).
[17]D. Dalacu, A. Kam, D. G. Austing, X. Wu, J. Lapointe, G. C. Aers, and P. J. Poole, Nanotechnology **20**, 395602 (2009).
[18]L. E. Fröberg, B. A. Wacaser, J. B. Wagner, S. Jeppesen, B. J. Ohlsson, K. Deppert, and L. Samuelson, Nano Lett. **8**, 3815 (2008).